

Theoretical Characterization of Nonlinear Clipping Effects in IM/DD Optical OFDM Systems

Liang Chen, Brian Krongold, and Jamie Evans

Abstract—This paper looks at the problem of theoretically characterizing the nonlinear biasing and clipping (BAC) effects on an optical Orthogonal Frequency-Division Multiplexing (OFDM) signal in intensity-modulated, direct-detected (IM/DD) optical systems. Due to the unipolarity of the IM/DD optical channel, a large DC bias and associated nonlinear clipping distortion (NLCD) is inevitable, resulting in a significant performance penalty. This NLCD can be well modelled as a linear deterministic attenuation plus an uncorrelated random additive clipping noise in the time domain. In the frequency domain, the NLCD results in an additive or impulsive noise on the received OFDM constellation. A total effective signal-to-noise ratio (SNR) formula is then presented which is a function of biasing power, modulation constellation and receiver SNR figure. This suggests that rather than eliminating all clippings, the system performance is indeed optimized with some deliberately introduced NLCD as a result of higher power efficiency. Analytical results are in agreement with simulations for various cases which help us to accurately and efficiently evaluate the performance of such systems.

Index Terms—Optical OFDM, intensity modulation, direct detection.

I. INTRODUCTION

DEMAND for ultra-high data rate optical communication services has grown tremendously in recent years. With an increased number of channels and/or bit rate, in conventional single-carrier optical systems it generally becomes impractical to completely remove the accumulated dispersion on all channels using a single dispersion-compensating fiber (DCF). Meanwhile, the computational complexity involved in electronic dispersion compensation (EDC) also becomes unacceptably high [1]. Therefore, in order to increase the throughput and allow more channels to transmit simultaneously, orthogonal frequency-division multiplexing (OFDM)

has emerged as one of the promising solutions to signal dispersion as it scales well with the data rate and/or transmission distance. Consequently, different flavors of optical OFDM systems have been proposed in either short-range free space [2]–[5], multi-mode fiber (MMF) [6]–[8], plastic optical fiber (POF) [9], [10] or long-haul single-mode fiber (SMF) systems [11]–[15].

An optical OFDM system, where the aggregate throughput is distributed over a large set of partially-overlapped yet orthogonal subchannels, is able to improve the immunity to turbulence and nonlinearities, as well as the tolerance to both chromatic [7] and polarization-mode dispersion [16]. Rather than trying to compensate the dispersion completely, optical OFDM intrinsically reduces the baud rate and, consequently, the amount of accumulated dispersion penalty. Unlike other traditional compensating methods where the signal can only be optimized for a single receiving point, information can be recovered in optical OFDM systems with minimal dispersion penalty anywhere along the link provided the dispersion is shorter than the cyclic prefix. With this manageable dispersion, transmit power can then be allowed to spread over a longer time scale, alleviating fiber nonlinearities during transmission. Even for traditional 10 or 40 Gb/s systems, it has been shown in [17] that employing OFDM can significantly reduce the capital expenditure of the network.

The modulating signal in optical OFDM systems is the output of the inverse fast Fourier transform (IFFT) and is bipolar in general. Thus, it cannot be directly applied to conventional intensity-modulated, direct-detected (IM/DD) systems that were previously designed for unipolar transmission, such as on-off keying (OOK) and pulse position modulation (PPM). For long-haul SMF systems, where the performance is limited by chromatic as well as polarization-mode dispersion, an optical single-sideband (OSSB) modulation with direct detector [11], [14] or a modified system with coherent transceivers [13], [15] have demonstrated the ability to minimize the dispersion penalty while also achieving a high spectral efficiency by providing an one-to-one frequency mapping between optical and electrical domains. While in short-range, free-space or MMF systems, which we are more interested in this paper, the achievable rate is largely limited by a combination of optical power and multipath dispersion. A more popular solution in this case is to use biasing followed by clipping (BAC) to simply transform the bipolar IFFT output into a unipolar signal [2], [4], [6]. The BAC method requires minimal modifications to existing IM/DD systems and hence is very attractive for its compactness and cost-effectiveness.

As the instantaneous envelope of the OFDM waveform

Paper approved by J. A. Salehi, the Editor for Optical CDMA of the IEEE Communications Society. Manuscript received March 2, 2011; revised September 25 and December 22, 2011.

This work is supported by National ICT, Australia (NICTA). NICTA is funded by the Australian Government as represented by the Department of Broadband, Communications and the Digital Economy and the Australian Research Council through the ICT Centre of Excellence program.

L. Chen and B. Krongold are with National ICT Australia, Victoria Research Laboratory and Department of Electrical and Electronic Engineering, University of Melbourne, Victoria 3010, Australia (e-mail: {lianchen, bsk}@unimelb.edu.au).

J. Evans is with the Department of Electrical and Computer Systems Engineering, Monash University, Victoria 3800, Australia (e-mail: jamie.evans@monash.edu).

This work was published in part in the Proceedings of the 2009 International Conference on Communications (ICC 2009), as “Performance Evaluation of Optical OFDM Systems with Nonlinear Clipping Distortion,” Dresden, Germany, June 2009.

Digital Object Identifier 10.1109/TCOMM.2012.060112.110136

generally follows a Gaussian distribution with a large peak-to-average power ratio (PAPR), the OFDM signal is very sensitive to nonlinear distortion. The transmission of such a signal is, thereby, largely limited by the linearity constraints in the modulation/demodulation processes, and by any nonlinear effects created on the unipolar IM/DD optical link. In order to avoid frequent nonlinear clipping of negative peaks, many previous works have assumed an *appropriate* and variable DC offset is added to eliminate clipping [4], [6]. However, it generally requires an average bias power of more than 10dB greater than the signal power. Since it is done either by inspection or, where necessary, exhaustive search over all data sequences, it is not particularly favorable for systems with a large number of subchannels. Other works have used fixed, yet large enough power to ensure an infrequent clipping from a statistical point of view. The authors in [2] applied a bias 9 dB greater than the r.m.s. value of the raw waveform. This number can be reduced in some cases by using windowing and pre-distortion [18] to achieve a balance between dynamic range and out-of-band distortion. The in-band distortion and/or symbol error rate (SER) degradation is, however, not considered. The bias can also be reduced via introducing dependence across subchannel symbols. By using a reserved subchannel set [19] or a block mapping scheme [20], the power efficiency can be greatly improved. But as a consequence, the total spectral efficiency is reduced. Furthermore, for a large IFFT size, the computational complexity of selecting the optimal symbol sequences for the data or reserved subchannel sets becomes prohibitively expensive as the candidate set grows exponentially. A trade-off between power and spectral efficiency has also been studied in [21]. By using only odd subchannels, the signal can be recovered noiselessly with 0-bias clipping, except for a 3-dB receiver sensitivity penalty. Clipping noise can be shown to fall onto even subchannels only, and half of the data subchannels are therefore abandoned. In the case of a real-valued IFFT output, the spectral efficiency is even lower. In order to deliver a similar rate as the above mentioned direct-biasing schemes, a much larger bandwidth and/or transmit power is required. The joint effect of quantization and clipping of an analog-to-digital converter is identified in [8], where the maximum achievable rates for certain links and photodetectors are presented by simulation. Searching for a universal optimal biasing power is also attempted through simulation in [7]. More recently, authors in [22] have further concluded that the optimal biasing/clipping level should also depend on the nonlinearities of the modulator as well as the D/A converter. However, these approaches did not provide theoretical insight into its relevance and dependence on modulation format and receiver parameters.

Notice although a large bias is desired to minimize the clipping distortion, it unfortunately does not contribute to the receiver signal-to-noise ratio (SNR) at all. In fact, through later discussion, we will see that a large biasing power can be detrimental to the overall performance. Furthermore, much of this research work is done only through simulation and without considering the dependence on modulation format and receiver sensitivity. Theoretical performance evaluation and optimization methods has received relatively little attention.

The remainder of this paper is outlined as follows: The

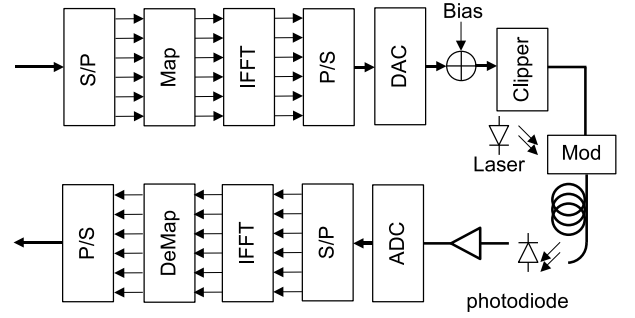


Fig. 1. An unamplified IM/DD optical OFDM system.

system model of an unamplified IM/DD optical OFDM system is presented in the next section, as well as an overview of some previous approaches. In Section III, we give a detailed analysis of some statistical properties of the BAC process which help us to model it as a linear deterministic attenuation plus a random additive clipping noise. Although the attenuation can easily be compensated at the receiver, the nonlinear clipping distortion (NLCD), which occurs in the time domain, through the receiver FFT process, results in distortions on all received symbols in the frequency domain. In section IV, the effect of this distortion on SER is analytically quantified and we present an effective SNR formula with respect to biasing power, modulation constellation and receiver SNR. An adaptive biasing strategy is identified which optimizes the clipping level and consequently minimizes the receiver SER and bit error rate (BER). Simulation results and related discussions are presented in Section V before we draw conclusions.

II. SYSTEM MODEL AND PROBLEM FORMULATION

A model of the short range IM/DD optical OFDM system considered here is shown in Fig. 1. At the transmitter, incoming high-speed data is first split into a large number of lower-speed data sets by a serial-to-parallel (S/P) converter before being encoded into QAM symbols and applied onto N equally-spaced subchannels. The complex symbols are then transformed into a time-domain signal via an IFFT, and the n -th sample of the output is given by

$$x_n = \frac{1}{N} \sum_{k=0}^{N-1} \left(X_k^I + jX_k^Q \right) \exp \left(j \frac{2\pi}{N} kn \right), \quad (1)$$

where $X_k^I + jX_k^Q$ is the complex symbol modulated on the k th subchannel. To focus on the effect of BAC, we look at the case where a real-valued signal is produced. Therefore, as in the case of digital multitone modulation [24], we enforce conjugate symmetry by setting $X_k^I = X_{N-k}^I$ and $X_k^Q = -X_{N-k}^Q$ for all $k < N/2$ except the first one. Notice in this case, only $N/2 - 1$ subchannels can be independently loaded. For the case of complex output, where all N subchannels are loaded with independent symbols, an intermediate (IM) frequency can be inserted to generate real waveforms via electronic I/Q modulation [11].

As the OFDM signal is the sum of a group of independent, identically distributed (i.i.d.) components, for any practical

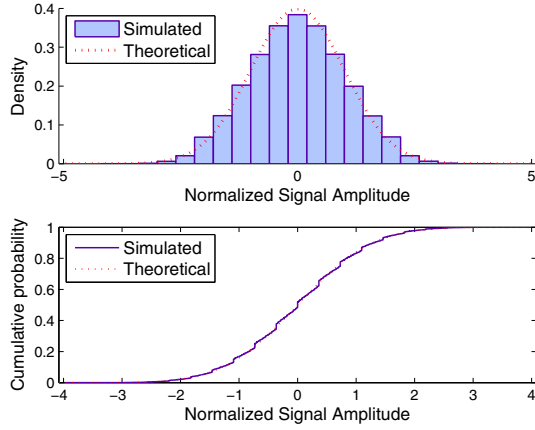


Fig. 2. Approximately Gaussian distributed time-domain OFDM signal.

choice of subchannel number and/or alphabet size, x_n becomes approximately Gaussian due to the central limit theorem. In the case of a real output, as a result of conjugate symmetric bit-loading, some correlation can be observed among x_n sequences. However, with a large subchannel number, $\{x_n\}$ can still be well approximated as i.i.d. Gaussian random variables [23]. Fig. 2 shows the time-domain characteristics of a simulated OFDM system with only 16 subchannels, each loaded with 4-QAM symbols. The output real baseband signal is first normalized so that the empirical variance is equal to one. Its probability density function (pdf) and cumulative distribution function (cdf) are then evaluated. The results suggest that we can accurately model the x_n sequence using an i.i.d. Gaussian process with the following pdf:

$$p_x(x) = \mathcal{N}(x; 0, \sigma^2), \quad (2)$$

where

$$\mathcal{N}(x; \mu, \sigma^2) \triangleq \frac{1}{\sqrt{2\pi}\sigma} e^{-\frac{(x-\mu)^2}{2\sigma^2}} \quad (3)$$

is a Gaussian distribution function with mean μ and variance σ^2 .

The output of the IFFT will then be transformed into a digital data sequence x_n by a parallel-to-serial (P/S) converter. A digital-to-analog converter (DAC) is used to convert this sequence into an analog waveform, which is generally bipolar. The BAC process is then employed so this signal can be delivered by a unipolar IM/DD system. With a simple rectangular pulse shaping function, if we denote the biasing voltage by I_{DC} , the equivalent asymmetrically-clipped time-domain samples x'_n (representing the output distorted signal sequence) are

$$x'_n = g(x_n) = \begin{cases} 0, & x_n < -I_{DC} \\ x_n + I_{DC}, & x_n \geq -I_{DC} \end{cases} \quad (4)$$

This helps in avoiding the complexity and high cost associated with an analog clipping device. In general, although the analog driving signal may still be negative after DAC, the effect is negligible [22]. This unipolar signal is then used to drive a linear optical modulator. For simplicity, we assume an ideal

intensity modulator is used here, where the instantaneous output optical power is a replica of the corresponding electrical-drive signal.

If the bias is set too low, the received signal will suffer from spectral spreading, intermodulation and harmonic generation due to the NLCD [25]. Due to the Gaussian nature of the waveform, in order to minimize clipping, a very large biasing power is needed, which will *NOT* contribute to the signal quality. This is due to the fact that both the IFFT and FFT processes can be effectively treated as vector summations, where the exponential terms in the summands are circularly symmetric, as shown in Eq. (1). Hence, when the input is a constant DC, the vector summation equals to 0. In fact, excessive biasing, which significantly increases the electronic driving power, is not always beneficial. If the maximum allowable input electronic and/or optical power for modulators, receivers, and/or amplifiers is limited (which is true for any practical system), by using a large electronic bias, the driving signal has to be shrunk by an automatic gain control (AGC) unit before being passed onto the modulator. Hence, the receiver electronic SNR will essentially decrease. In fact, later we show that for any practical system with a specific modulation format and receiver sensitivity figure, there exists an optimal biasing point where the SER/BER can be minimized. The objective of this paper is to develop a theoretical performance analysis and consequently optimize the receiver performance with regards to both modulation format and receiver SNR.

III. STATISTICAL PROPERTIES OF CLIPPED SIGNAL

Due to the circular symmetry of the IFFT, subtracting any DC component from the received signal will not affect the OFDM receiver performance. Therefore, without loss of generality, if the original bias point is shifted to zero, i.e., $y_n = x'_n - I_{DC}$, the BAC process is indeed equivalent to a single-sided Cartesian clipper, similar to those considered in [26], [27], except for its asymmetry. The mean of the equivalent output signal y_n can be calculated as

$$\begin{aligned} \mu_y &= E[g(x)] - I_{DC} = \int_{-I_{DC}}^{\infty} (x + I_{DC}) p_x(x) dx - I_{DC} \\ &= \int_{-I_{DC}}^{\infty} \frac{x}{\sqrt{2\pi}\sigma} e^{-\frac{x^2}{2\sigma^2}} dx - I_{DC} \left(1 - \int_{-I_{DC}}^{\infty} \frac{1}{\sqrt{2\pi}\sigma} e^{-\frac{x^2}{2\sigma^2}} dx \right) \\ &= \frac{\sigma}{\sqrt{2\pi}} e^{-\frac{I_{DC}^2}{2\sigma^2}} - I_{DC} Q\left(\frac{I_{DC}}{\sigma}\right), \end{aligned} \quad (5)$$

where the well known Q -function is defined as the integral over normal pdf

$$Q(\nu) \triangleq \int_{\nu}^{\infty} \mathcal{N}(\tau; 0, 1) d\tau \triangleq 1 - \Phi(\nu). \quad (6)$$

Thus, y_n is not a zero-mean random signal anymore and its variance can be described as

$$\begin{aligned} \sigma_y^2 &= E[y_n^2] - \mu_y^2 = \int_{-I_{DC}}^{-I_{DC}} I_{DC}^2 p_x(x) dx + \int_{-I_{DC}}^{+\infty} x^2 p_x(x) dx - \mu_y^2 \\ &= \sigma^2 + (I_{DC}^2 - \sigma^2) Q\left(\frac{I_{DC}}{\sigma}\right) - I_{DC}^2 \left[Q\left(\frac{I_{DC}}{\sigma}\right) \right]^2 \dots \end{aligned}$$

$$-\frac{\sigma^2}{2\pi} e^{-\frac{I_{DC}^2}{\sigma^2}} - \frac{\sigma I_{DC}}{\sqrt{2\pi}} e^{-\frac{I_{DC}^2}{2\sigma^2}} \left[1 - 2Q\left(\frac{I_{DC}}{\sigma}\right) \right]. \quad (7)$$

Although the statistical properties of Y can be explicitly described, the error probability of such a system is still hard to derive due to the nonlinear nature of the BAC process. Therefore, for the upcoming analysis, it is desirable to decompose the memoryless nonlinear BAC effect into a linear process with a deterministic attenuation K plus a random time-domain additive clipping noise (TD-CN) z_n

$$y_n = Kx_n + z_n. \quad (8)$$

Furthermore, we are interested in the case where the clipping noise z_n is carefully chosen to be uncorrelated with the input signal x_n , i.e., $E[z_n x_n] = E[(y_n - Kx_n)x_n] = 0$.

Notice that if we subtract μ_y , the mean of the clipped output, from both sides of Eq.(8) and then denote $y'_n = y_n - \mu_y$ and $z'_n = z_n - \mu_y$, the above equation can be rewritten as

$$y'_n = Kx_n + z'_n, \quad (9)$$

where x_n , y'_n and z'_n are all zero-mean random variables and $E[z'_n x_n] = 0$.

In order to find the best linear mean square error (LMMSE) approximation, we multiply both sides of the above equation by x_n , so that $x_n y'_n = Kx_n^2 + z'_n x_n$. Therefore, the clipping attenuation K , which represents the slope of the linear approximation, can be chosen so that

$$\begin{aligned} K &= \frac{E[(y'_n)x_n]}{E[x_n x_n]} = \frac{E[(y_n - \mu_y)x_n]}{E[x_n^2]} \\ &= \frac{1}{\sigma^2} \int_{-\infty}^{+\infty} [g(x) - \mu_y] x p_x(x) dx \\ &= 1 - Q\left(\frac{I_{DC}}{\sigma}\right) = \Phi\left(\frac{I_{DC}}{\sigma}\right). \end{aligned} \quad (10)$$

Since x_n is zero mean, the mean of the random uncorrelated TD-CN z_n is then as follows

$$\mu_z = E[Y - KX] = \mu_y - KE[X] = \mu_y. \quad (11)$$

The variance of z_n also can be calculated via the difference between the input and output power

$$\begin{aligned} \sigma_z^2 &= \sigma_y^2 - K^2 \sigma^2 \\ &= \sigma^2 \left\{ (1 + \gamma^2) [Q(\gamma) - Q^2(\gamma)] - \frac{1}{2\pi} e^{-\gamma^2} \dots \right. \\ &\quad \left. - \frac{\gamma}{\sqrt{2\pi}} e^{-\frac{\gamma^2}{2}} [1 - 2Q(\gamma)] \right\}, \end{aligned} \quad (12)$$

where $\gamma = I_{DC}/\sigma$ is the normalized clipping level, and is independent of the number of subchannels in the system.

Thus, the nonlinear BAC process can be effectively modelled as a deterministic attenuation K and uncorrelated additive noise z_n with variance σ_z^2 , both depending on only the normalized bias level γ and can easily be calculated.

IV. EFFECTS OF CLIPPING IN FREQUENCY DOMAIN

The output signal $x'_n = y_n + I_{DC}$ is used to drive a linear modulator and the output optical beam will then travel through a channel suffering from various attenuations, dispersion and nonlinear effects before the distorted signal hits the receiver where it may again be corrupted by electronic noise. Since IM/DD optical OFDM has shown a strong tolerance to both attenuation and dispersion, in order to evaluate the methodology in this paper, we look at a simple case where losses and dispersion accumulated along the optical path can be fully compensated, and nonlinearities and ASE noises are not included. This is a suitable model for short range MMF, optical wireless and POF transmission, and system performance is thereby limited mainly by the nonlinear clipping at the transmitter and noise at the receiver.

A zero-mean Gaussian noise process e_n with variance σ_n^2 is used to denote the joint effect of various noise processes which may be presented at the receiver side. Though, it would be clear through later discussion that the methodology we presented can be used for systems with multiple additive noise/distortion sources, e.g., ADC quantization noises. Under this assumption, the received signal is

$$\tilde{y}_n = x'_n + e_n \approx Kx_n + z_n + I_{DC} + e_n. \quad (13)$$

Since the DC bias term I_{DC} will be cancelled out, the detected signal passing through the OFDM FFT demodulator results in an attenuated signal and two noise terms in each subchannel,

$$\begin{aligned} \tilde{X}_k &= \tilde{X}_k^I + j\tilde{X}_k^Q \\ &\approx K \left(X_k^I + jX_k^Q \right) + \left(r_k^I + jr_k^Q \right) + \left(n_k^I + jn_k^Q \right), \end{aligned} \quad (14)$$

where n_k is the frequency-domain additive noise attributed from e_n with the same variance σ_n^2 , and r_k is the frequency-domain additive clipping noise (FD-CN) due to time-domain BAC process

$$r_k = r_k^I + jr_k^Q = \sum_{n=0}^{N-1} z_n \exp\left(-j\frac{2\pi}{N}kn\right). \quad (15)$$

When the clipping level γ is set sufficiently low to produce several clipping events per OFDM symbol, Eq. (15) can be viewed as a linear combination of N i.i.d. random variables. Thus, its pdf can be well approximated as a Gaussian function with variance σ_z^2 , especially for large N . When γ is high, the central limit theorem cannot be invoked as clipping becomes a rare event. In this case, the FD-CN is better modelled as impulsive noise [27], [29]. However, the later one has only negligible impact on the system performance and additive FD-CN, in general, provides a simple evaluation with reasonable accuracy.

A. Clipping Attenuation

The clipping attenuation K in Eq. (14) results in a shrinking of the decision regions for the received signal constellations. Although it may not have any effect for systems using BPSK or QPSK/4-QAM modulation, where only the phase information is collected for decision, for any other higher-order modulation schemes, compensating this clipping attenuation can significantly improve the system performance.

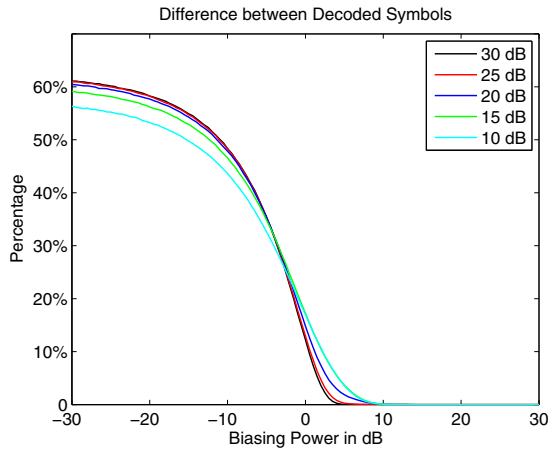


Fig. 3. Percentage of symbol difference after compensating the clipping attenuation for different receiver SNRs.

Fig. 3 shows the difference between decoded symbols with and without considering the clipping attenuation K in a simulated IM/DD optical OFDM system with 1024 sub-channels and 16-QAM modulation. Different biasing power and receiver SNR figures are also tested. We see that after compensation, up to 60% of QAM symbols could be decoded differently. With an increased bias, as $K = 1 - Q(\gamma)$ quickly approaches 1, the percentage of this difference drops to zero accordingly. It is important to note that a difference between decoded symbols, does not always correspond to a decoding error, because the signal recovery also depends on the clipping level and receiver noises. Therefore, as shown in Fig. 4, although a similar percentage of difference for different receiver SNR can be observed, the SER improvement is quite different. For high SNR, up to 38% of the errors can be corrected via K compensation without any extra transmit power or hardware. For low biasing levels, a strong clipping noise r_k results in most of the received symbols falling out of the decision region with the attenuation factor K around 0.5. The improvement on the SER via K compensation is quite steady around 25%. With an increased biasing level, K quickly approaches to 1. Receiver noise then becomes the dominant performance limiter. As a result, this improvement increases slowly to its maximum point and then quickly drops to zero for large bias.

B. Effective Receiver SNR

Due to the large DC bias added in during the BAC process, the signal power is significantly increased. As a result, x'_n cannot normally be directly applied onto the modulator without an AGC. Hence, in the region where the receiver noise starts to dominate, excessive biasing will eventually reduce the effective received electronic SNR. The purpose of this section is to find the optimal biasing point that achieves a maximized SNR with both an electronic and optical power constraint.

1) *With Limited Electrical Power:* After the BAC process, the overall signal electrical power becomes $\sigma_y^2 + I_{DC}^2$. Without loss of generality, it is assumed here that the maximum

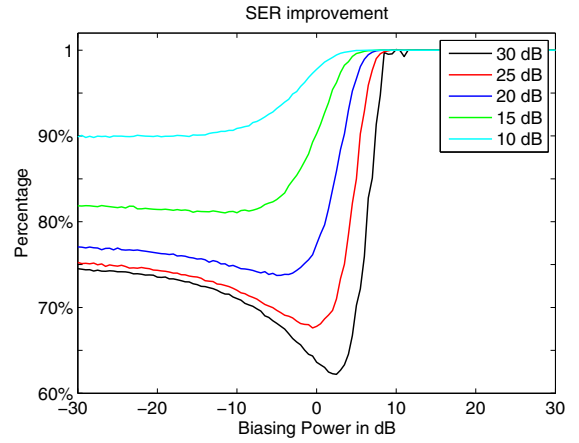


Fig. 4. Percentage of symbol error rate after compensating the clipping attenuation for different receiver SNRs.

electronic power the modulator can handle is unity.¹ Again, since the DC component in x'_n is not bearing any information and will be canceled out after receiver FFT, the effective driving signal y'_n after normalization is then

$$y'_n = \frac{x'_n - I_{DC}}{\sqrt{\sigma_y^2 + I_{DC}^2}} \approx \frac{x'_n - \gamma\sigma}{\sqrt{\sigma^2 + I_{DC}^2}} = \frac{y_n}{\sigma\sqrt{1+\gamma^2}}. \quad (16)$$

Notice that for small biasing, a significant amount of power will be clipped out, and hence, $E[x_n'^2] < (1 + \gamma^2)\sigma^2$. In general, however, Eq. (16) provides a good approximation.

Consequently, the received symbol \tilde{X}_k , which is previously expressed in Eq. (14), becomes $\frac{K}{\sigma\sqrt{1+\gamma^2}}X_k + \frac{1}{\sigma\sqrt{1+\gamma^2}}r_k + n_k$. In order to further optimize the receiver SER with regards to both K and σ_z^2 , we define the effective signal-to-total-noise ratio (SNR) as the ratio between the signal power and the sum power of both the clipping noise and receiver noise. Under the electrical power constraint, it can be expressed as

$$\begin{aligned} \text{SNR}^E &= \frac{K^2 E[|X_k|^2] / [(1 + \gamma^2)\sigma^2]}{E[|r_k|^2] / [(1 + \gamma^2)\sigma^2] + E[|n_k|^2]} \\ &= \frac{K^2 \sigma^2 / (1 + \gamma^2)}{\sigma_z^2 / (1 + \gamma^2) + \sigma^2 \sigma_n^2}. \end{aligned} \quad (17)$$

Notice that in the above equation, instead of using $E[|z_n|^2]$, the clipping noise power is measured by σ_z^2 . This is because the DC power contained in z_n , will not contribute to SNR due to the circular symmetry of the FFT. For the same reason, the transmitted-signal-to-clipping-noise ratio can be defined as $\text{SNR}_c = \frac{K^2 \sigma^2}{\sigma_z^2}$. The received-signal-to-receiver-noise ratio is then defined as $\text{SNR}_d = \frac{\sigma_y^2}{\sigma_n^2}$, so that it is independent from the power normalization. Consequently, the effective receiver SNR^E becomes

$$\text{SNR}^E = \frac{\text{SNR}_c \text{SNR}_d}{(1 + \text{SNR}_c)(1 + \gamma^2)\sigma^2 + \text{SNR}_d}. \quad (18)$$

¹Notice that this maximum can be any arbitrary fixed value, while the choice we have here helps us to simplify the SNR expression. If instead, the maximum is set to ϵ , an additional constant scaling factor of ϵ is then needed in Eq. (17); the overall analysis presented in this paper, however, remains the same.

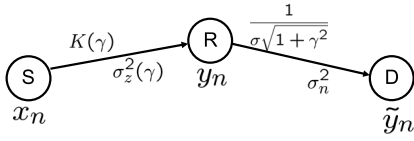


Fig. 5. Asymmetric clipping as an amplify-and-forward relay.

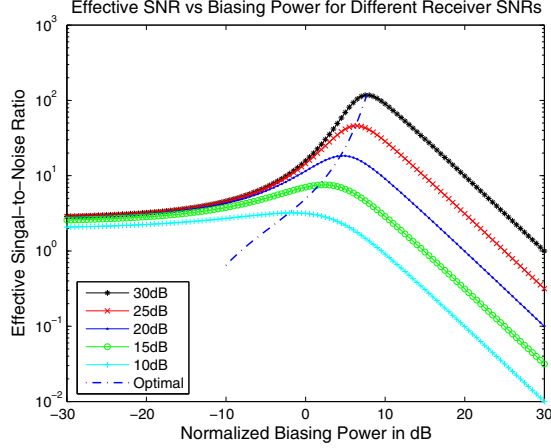


Fig. 6. Biasing power vs. total effective SNR for different receiver SNRs.

This result is very similar to what has been observed for a single-hop, full-duplex, amplify-and-forward relay network. Or in other words, as shown in Fig. 5, the BAC process can be modelled as a virtual channel from the source node (S) to the relay node (R) with attenuation K and noise power σ_z^2 , both of which are functions of only γ . The normalization process and the following AWGN channel are then modelled as a virtual channel from the relay node (R) to the destination (D) with attenuation $\frac{1}{\sigma\sqrt{1+\gamma^2}}$ and noise power σ_n^2 . The methodology can then be easily extended to a system with multiple additive noises and/or distortion sources by adding more virtual relay nodes along the path.

Eq. (18) is not a monotonic function of γ , and for a very small biasing power, $\text{SNR}_c \ll \text{SNR}_d$, the effective SNR^E becomes

$$\text{SNR}^E = \frac{\text{SNR}_c}{\frac{(1+\text{SNR}_c)(1+\gamma^2)\sigma^2}{\text{SNR}_d} + 1} \approx \text{SNR}_c. \quad (19)$$

By increasing the biasing power for this region, SNR_c as well as the total effective SNR^E begin to increase, thereby leading to a decreased SER.

On the other hand, with a very large biasing power, $\text{SNR}_c \gg \text{SNR}_d$, and the total SNR^E is approximated as

$$\begin{aligned} \text{SNR}^E &= \frac{\text{SNR}_d}{\frac{(1+\text{SNR}_c)}{\text{SNR}_c}(1+\gamma^2)\sigma^2 + \frac{\text{SNR}_d}{\text{SNR}_c}} \\ &\approx \frac{\text{SNR}_d}{(1+\gamma^2)\sigma^2} \leq \frac{1}{(1+\gamma^2)\sigma_n^2}, \end{aligned} \quad (20)$$

where the last approximation is due to the fact that σ_y^2 approaches σ^2 for large biases. In this case, by increasing the biasing power, the effective SNR^E starts to decrease since the received signal contains a very large DC component. Consequently, the SER increases.

TABLE I
OPTIMIZED SYSTEM PERFORMANCE FOR DIFFERENT RECEIVER SNRS.

Rec. SNR (dB)	10	15	20	25	30
Opt. Bias γ^*	0.8588	1.2692	1.6818	2.0686	2.4247
Max. SNR (dB)	5.706	9.2163	12.875	16.732	20.764
Min. SER	0.497	0.272	0.072	0.0032	1.56e-006
No. Iterations	12	11	10	13	14
Time (ms)	5.1898	2.9582	4.8155	3.2104	3.3495

Fig. 6 shows the result of effective receiver SNR^E versus biasing power for a simulated optical OFDM system after BAC. For each receiver, as expected, there exists an optimal biasing point. With an increased receiver SNR, this optimal biasing power is increased as well.

In order to maximize the system performance, which is equivalent to finding the optimal biasing point that maximizes the effective SNR, Eq. (18) is rewritten as

$$\text{SNR}^E = \frac{\text{SNR}_d}{\frac{(1+\text{SNR}_c)}{\text{SNR}_c}(1+\gamma^2)\sigma^2 + \frac{\text{SNR}_d}{\text{SNR}_c}}. \quad (21)$$

Since the numerator is a constant, the objective is therefore to minimize the denominator. Applying the golden section search with parabolic interpolation [30], optimum values can easily be found as shown in the dashed line in Fig. 6.²

Eq. (18) does not depend on the number of subchannels and modulation constellations. Thereby, the proposed searching algorithm has a low and stable computational complexity. For practical implementation, a lookup table can be constructed prior to online operation. Table I shows some of the key results and performance parameters obtained using Matlab on a standard P4 desktop. Due to the AGC, the maximum effective SNR is always smaller than receiver SNR.

2) *With limited optical power:* In IM/DD optical OFDM systems, the optical intensity modulator generates an optical output signal with intensity (not amplitude or voltage) proportional to x'_n (not $x_n'^2$). The main system constraint in many cases is then the average optical transmitting power, while the performance of the OFDM signal depends on the effective SNR of the electronic signal after receiver detection.

Note that for a given signal, its optical power depends on its mean, while its electrical power depends on its second moment. Without any normalization, the output optical power of the modulator is then $\mu_y + I_{DC}$. Again, without loss of generality, it is assumed here that the maximum optical output power of the optical modulator is unity. The effective driving signal y'_n after normalization is then

$$y'_n = \frac{x'_n - I_{DC}}{\mu_y + I_{DC}} \approx \frac{x'_n - \gamma\sigma}{I_{DC}} = \frac{y_n}{\gamma\sigma}. \quad (22)$$

Again, for small biasing, as a significant amount of power will be clipped out, $E[x'_n] < \gamma\sigma$. In general, however, Eq. (22) provides a good approximation.

The received symbol \tilde{X}_k then becomes $\frac{K}{\gamma\sigma}X_k + \frac{1}{\gamma\sigma}r_k + n_k$. The effective SNR^O under an optical power constraint is then

²For extremely poor receivers, the optimal point seems to drift away from the peak a little due to the normalization error in Eq. (16). However, these points are out of the region we are interested in.

as follows:

$$\begin{aligned} \text{SNR}^O &= \frac{K^2 E[|X_k|^2] / (\gamma^2 \sigma^2)}{E[|r_k|^2] / (\gamma^2 \sigma^2) + E[|n_k|^2]} = \frac{K^2 / \gamma^2}{\sigma_z^2 / \gamma^2 + \sigma^2 \sigma_n^2} \\ &= \frac{\text{SNR}_c \text{SNR}_d}{(1 + \text{SNR}_c) \gamma^2 \sigma^2 + \text{SNR}_d}. \end{aligned} \quad (23)$$

This result is very similar to Eq. (18), indicating that for systems with both electronic or optical power constraints, there exists optimal biasing points for which the received electronic SNR can be maximized, and the methodology we presented above can easily be modified to accommodate both cases with similar performance.

C. Adaptive Biasing

Unlike the previous approaches, the proposed optimization method is not focused on eliminating all the clipping, but rather to provide a *sufficient* bias so that the clipping noise z_n is not the dominant noise source in the system. Again, if the input signal x_n is modelled as an i.i.d. Gaussian process, the probability that an IFFT output sample gets clipped under optimal bias voltage $\gamma^* \sigma$ is

$$P_s = \Pr(x_n < -\gamma^* \sigma) = \int_{-\infty}^{-\gamma^*} \mathcal{N}(\tau; 0, 1) d\tau = Q(\gamma^*), \quad (24)$$

which is independent of subchannel numbers or modulation schemes. The optimized probability that an IFFT output symbol gets clipped can then be approximated as

$$P_S = 1 - \prod_{k=0}^{N-1} \Pr(x_n > -\gamma^* \sigma) = 1 - [1 - Q(\gamma^*)]^N. \quad (25)$$

Fig. 7 shows the simulated results obtained for an IM/DD optical OFDM transmission with different receiver SNR figures. In all cases, the IFFT output x_n is biased using the optimal bias found in Fig. 6 and then clipped to eliminate any remaining negative peaks. With a fixed signal power of σ^2 on all available subchannels, we analyze both sample and symbol clipping probabilities with various choices of N . For a given bias $\gamma^* \sigma$, the sample clipping probability is independent of the number of subchannels N and modulation format M . The symbol clipping probability curve for a system equipped with a larger-sized IFFT is much steeper, thereby indicating a higher probability of having all symbols clipped for a wide range of receiver SNR.

Therefore, for systems using a small number of transmitting subchannels and a high SNR receiver, not all symbols will be clipped, even with the optimal biasing. Thus, the normalized adaptive bias for a single IFFT output can be chosen as follows:

$$\gamma = \min \left\{ \gamma^*, \frac{|\min[\min(x_n), 0]|}{\sigma} \right\}, \quad (26)$$

where the average bias can be further reduced to

$$E[\gamma] = \sigma \left(P_S \cdot \gamma^* - N \int_{-\gamma^*}^0 [\Phi(\gamma)]^{N-1} \Phi'(\gamma) \gamma d\gamma \right). \quad (27)$$

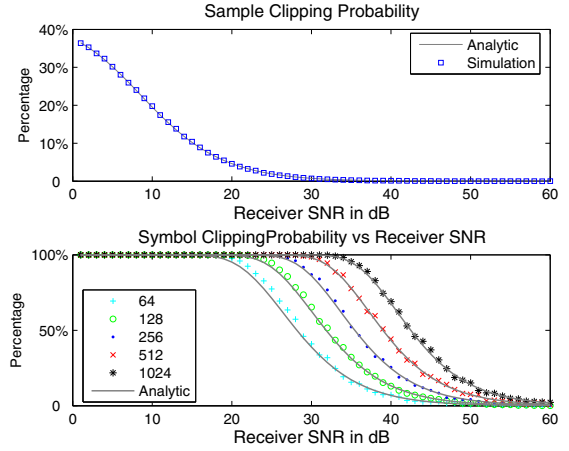


Fig. 7. Sample (a) and symbol (b) clipping probabilities.

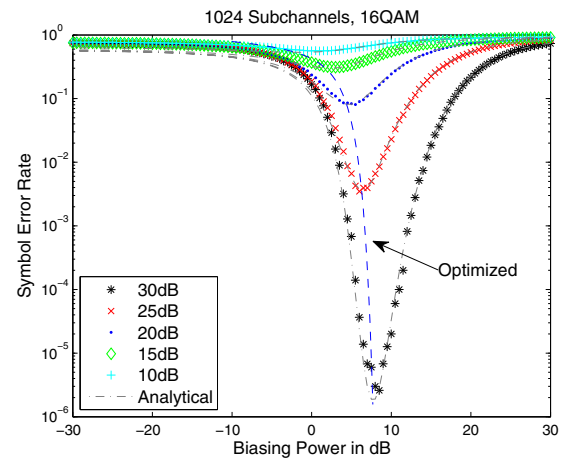


Fig. 8. SER versus biasing power for different receiver SNRs.

Using Eq. (18) and Eq. (23), performance of such systems can be evaluated theoretically. For example, the SER of a M -QAM direct-detected optical OFDM system with clipping can be derived by the classical approach [31]

$$P_b = 1 - \left[1 - 2 \left(1 - \frac{1}{\sqrt{M}} \right) Q \left(\sqrt{\frac{3}{M-1} \text{SNR}} \right) \right]^2, \quad (28)$$

which will then be a function of biasing level γ , modulation format M and SNR_d , the receiver SNR.

V. SIMULATION RESULTS

We analyze the performance of an IM/DD optical OFDM system with 1024 subchannels, each loaded with 16-QAM complex symbols. The maximum electrical power at the transmitter is set to unity. To determine the optimal biasing level, 1,000,000 random binary bits are tested with various biasing powers. The optical attenuation and dispersion is fully compensated so that we can focus on the effect of the BAC process. Fig. 8 shows the SER curve for 5 different receivers. The dash line in the middle represents the analytical result of minimized SER under optimal bias, which achieves an excellent agreement with the simulation results. For a small biasing power, the dominant noise source is the clipping noise

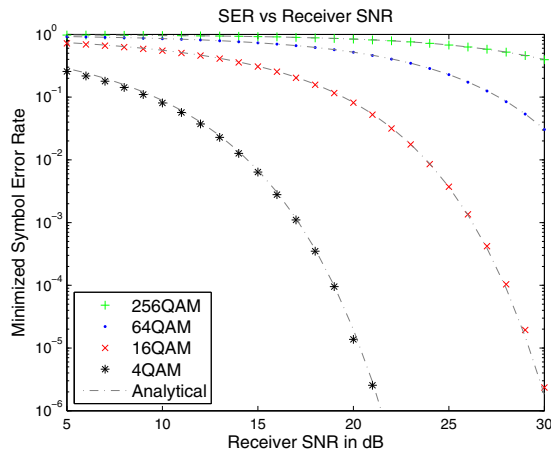


Fig. 9. SER versus receiver SNR for different modulations.

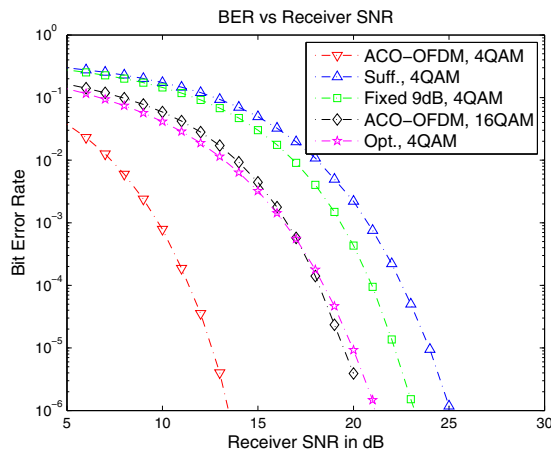


Fig. 10. BER versus receiver SNR for different biasing strategies.

due to BAC. Therefore, the SER difference between different receivers is negligible. The most effective way to improve the system performance in this case is to increase the biasing power. However, for a large biasing power, the dominant source becomes the receiver noise. The most effective way to improve the system performance here is to use a better receiver, though a better receiver with a higher SNR figure tends to require an even higher optimal biasing power. Similar results can be observed for different modulation schemes and for the optical-power-constrained cases, where the optimal bias level is then simply $\sqrt{1 + \gamma^*^2}$.

The value of optimal bias that maximizes the effective SNR is independent from the choice of the constellation size. Hence, with the proposed search algorithm, similar performance can be achieved for systems loaded with 4/16/64/256-QAM, as shown in Fig. 9.

Finally, we compare the power efficiencies across systems with different biasing strategies. In making a fair comparison, we assume that the signal bandwidth for all OFDM systems is limited within the same range. For all systems loaded with 4-QAM symbols, sufficiently biased OFDM (denoted by “Suff.” in the plot) requires the largest transmitting power while the ACO-OFDM systems [21] requires the least amount of power. Note that since only odd subchannels can be loaded to form

the anti-periodic driving signal, in order to achieve a same bit rate without increasing the bandwidth, a larger constellation of 16-QAM is required. Fixed biased systems uses a fixed bias of 9 dB throughout the whole region (denoted by “Fixed 9dB” in the Figure) is over-biased in this case. Optimal biased system we proposed in this paper (denoted by “Opt.” in the Figure) is the most power efficient one, except in the very low BER regions where the ACO-OFDM is slightly better. Compared to sufficiently biased and fixed biased systems, by optimizing the electronic bias, the receiver sensitivities can be improved by around 4 dB and 2 dB respectively.

VI. CONCLUSION

By applying a MMSE linear approximation to the biasing and clipping process, the nonlinear process can essentially be modeled as a virtual relay channel. This idea can easily be extended to systems with multiple additive noises/distortions. The effect of clipping on the time-domain signal can then be effectively separated into a deterministic attenuation and an uncorrelated noise on the received frequency-domain constellation. Using the total effective SNR formula, an optimal biasing point that maximizes the effective SNR can be determined with the proposed fast searching algorithm. This algorithm is not focused on eliminating all the clipping, but rather to provide an optimized bias so that the clipping distortion is no longer the dominant noise source. The proposed optimal biasing strategy does not require any online calculation and can be used in different optical channels with different receiver figures and modulation methods.

REFERENCES

- [1] H. Bulow, F. Buchali, and A. Klekamp, “Electronic dispersion compensation,” *IEEE J. Lightwave Technol.*, vol. 26, no. 1, pp. 158–167, Jan. 2008.
- [2] O. Gonzalez, R. Perez-Jimenez, S. Rodriguze, J. Rabadan, and A. Ayala, “OFDM over indoor wireless optical channel,” *IEE Proc. Optoelectron.*, vol. 152, no. 4, pp. 199–204, 2005.
- [3] N. Cvijetic, D. Qian, and T. Wang, “10Gb/s free-space optical transmission using OFDM,” in *Proc. 2008 OFC/NFOFC, OThD2*. I. B. Djordjevic, B. Vasic, and M. A. Neifeld, “LDPC coded OFDM over the atmospheric turbulence channel,” *Optics Express*, vol. 15, pp. 6336–6350, May 2007.
- [4] J. Carruthers and J. Kahn, “Multi-subcarrier modulation for non-directed wireless infrared communication,” *IEEE J. Sel. Areas Commun.*, vol. 14, no. 3, pp. 538–546, Apr. 1996.
- [5] S. Hashemi, Z. Ghassemlooy, L. Chao, and D. Benhaddou, “Orthogonal frequency division multiplexing for indoor optical wireless communications using visible light LEDs,” in *Proc. 2008 CNSDSP*, pp. 174–178.
- [6] S. Randel, F. Breyer, and S. Lee, “High-speed transmission over multimode optical fibers,” in *Proc. 2008 OFC/NFOFC, OWR2*.
- [7] I. Djordjevic, B. Vasic, and M. Neifeld, “LDPC-coded OFDM for optical communication systems with direct detection,” *IEEE J. Sel. Topics Quantum Electron.*, vol. 13, no. 5, pp. 1446–1454, Sep./Oct. 2007.
- [8] J. M. Tang and K. A. Shore, “Maximizing the transmission performance of adaptively modulated optical OFDM signals in multimode-fiber link by optimizing analog-to-digital converter,” *IEEE J. Lightwave Technol.*, vol. 25, no. 3, pp. 787–798, Mar. 2007.
- [9] S. Lee, F. Breyer, S. Randel, O. Ziemann, H. van den Boom, and A. Koonen, “Low-cost and robust 1-Gbit/s plastic optical fiber link based on light-emitting diode technology,” in *Proc. 2008 OFC/NFOFC, OWB3*.
- [10] S. Lee, F. Breyer, S. Randel, R. Gaudino, G. Bosco, A. Bluschke, M. Matthews, P. Rietzsch, R. Steglich, H. van de Boom, and A. Koonen, “Discrete multitone modulation for maximizing transmission rate in step-index plastic optical fibers,” *IEEE J. Lightwave Technol.*, vol. 27, no. 11, pp. 1503–1513, Nov. 2009.

- [11] A. J. Lowery, L. Du, and J. Armstrong, "Performance of optical OFDM in ultralong-haul WDM lightwave systems," *IEEE J. Lightwave Technol.*, vol. 25, no. 1, pp. 131–138, Jan. 2007.
- [12] W. Shieh and C. Athaudage, "Coherent optical orthogonal frequency division multiplexing," *IEEE Electron. Lett.*, vol. 42, no. 10, pp. 587–588, 2006.
- [13] S. Jansen, I. Morita, T. Schenk, N. Takada, and H. Tanaka, "Coherent optical 25.8-Gb/s OFDM transmission over 4160-km SSMF," *IEEE J. Lightwave Technol.*, vol. 26, no. 1, pp. 6–15, Jan. 2008.
- [14] B. Schmidt, A. Lowery, and J. Armstrong, "Impact of PMD in single-receiver and polarization-diverse direct-detection optical OFDM," *IEEE J. Lightwave Technol.*, vol. 27, no. 14, pp. 2792–2799, Nov. 2009.
- [15] Y. Ma, Q. Yang, Y. Tang, S. Chen, and W. Shieh, "1-Tb/s single-channel coherent optical OFDM transmission with orthogonal-band multiplexing and subwavelength bandwidth access," *IEEE J. Lightwave Technol.*, vol. 28, no. 4, pp. 308–315, Feb. 2010.
- [16] W. Shieh, W. Chen, and R. Tucker, "Polarisation mode dispersion mitigation in coherent optical orthogonal frequency division multiplexed systems," *IEEE Electron. Lett.*, vol. 42, no. 17, pp. 996–997, Apr. 2006.
- [17] A. Bocoi, M. Rambach, D. Schupke, C.-A. Bunge, and B. Spinnler, "Cost comparison of networks using traditional 10 and 40 Gb/s transponders versus OFDM transponders," in *Proc. 2008 OFC/NFOFC, OThB4*.
- [18] D. Chanda, A. Sesay, and B. Davies, "Performance of clipped OFDM signal in fiber," in *Proc. 2004 IEEE Canadian Conf. Electr. Comput. Eng.*, vol. 4, pp. 2401–2404.
- [19] R. You and J. Kahn, "Average power reduction techniques for multiple subcarrier intensity-modulated optical signals," *IEEE Trans. Commun.*, vol. 49, no. 12, pp. 2164–2171, Dec. 2001.
- [20] S. Teramoto and T. Ohtsuki, "Multiple-subcarrier optical communication systems with subcarrier signal-point sequence," *IEEE Trans. Commun.*, vol. 53, no. 10, pp. 1738–1743, Oct. 2005.
- [21] J. Armstrong and A. Lowery, "Power efficient optical OFDM," *IEEE Electron. Lett.*, vol. 42, no. 6, pp. 370–372, Mar. 2006.
- [22] D. Barros and J. Kahn, "Optical modulator optimization for orthogonal frequency-division multiplexing," *IEEE J. Lightwave Technol.*, vol. 27, no. 13, pp. 2370–2378, July 2009.
- [23] L. Chen, "Distortion management in intensity modulated optical OFDM systems," Ph.D. dissertation, University of Melbourne, 2012.
- [24] J. Chow, J. Tu, and J. Cioffi, "A discrete multitone transceiver system for HDSL applications," *IEEE J. Sel. Areas Commun.*, vol. 9, no. 6, pp. 895–908, Aug. 1991.
- [25] H. Ochiai and H. Imai, "Performance analysis of deliberately clipped OFDM signals," *IEEE Trans. Commun.*, vol. 50, no. 1, pp. 89–101, Jan. 2002.
- [26] K.-P. Ho and J. Kahn, "Optimal predistortion of Gaussian inputs for clipping channels," *IEEE Trans. Commun.*, vol. 44, no. 11, pp. 1505–1513, Nov. 1996.
- [27] H. Nikopour and S. Jamali, "On the performance of OFDM systems over a cartesian clipping channel: a theoretical approach," *IEEE Trans. Wireless Commun.*, vol. 3, no. 6, pp. 2083–2096, Nov. 2004.
- [28] A. Papoulis, *Probability, Random Variables, and Stochastic Processes*. McGraw-Hill, 1984.
- [29] A. Bahai, M. Singh, and A. Goldsmith, "A new approach for evaluating clipping distortion in multicarrier systems," *IEEE J. Sel. Areas Commun.*, vol. 20, no. 5, pp. 1037–1045, June 2002.
- [30] R. Brent, *Algorithms for Minimization without Derivatives*. Prentice-Hall, 1973.
- [31] J. Proakis, *Digital Communications*. McGraw-Hill Higher Education, 2001.



Australian. His current research interests include signal processing for both wireless and optical orthogonal frequency-division multiplexing (OFDM) systems.



Research Fellowship and held this from 2005 to 2008. Since January 2008 he has been a Senior Lecturer at the University of Melbourne.

During the summer of 1994, he interned for Martin Marietta at the Oak Ridge National Laboratory, Oak Ridge, Tennessee. From January to August 1995, he consulted at Bell Laboratories in Middletown, New Jersey. During the summer of 1998, he worked at the Electronics and Telecommunications Research Institute, Taejon, South Korea, under a National Science Foundation summer research grant. During the first half of 2011, he was on sabbatical at Alcatel-Lucent Bell Laboratories in Murray Hill, New Jersey. He received second prize in the Student Paper Contest at the 2001 Asilomar Conference on Signals, Systems, and Computers, and the Best Paper Award at the 2006 European Wireless Conference. His work on active constellation extension for OFDM PAPR reduction is part of the DVB-T2 digital video broadcast standard. His current research interests are in multicarrier communications systems, energy-efficient communications, and signal processing for optical communications.



Department of Electrical Engineering and Computer Science, University of California, Berkeley. He returned to Australia to take up a position as Lecturer at the University of Sydney, Australia, where he stayed until July 2001. From July 2001 until March 2012 he was with the Department of Electrical and Electronic Engineering, University of Melbourne. He is currently a Professor in the Department of Electrical and Computer Systems Engineering at Monash University, Australia. His research interests are in communications theory, information theory, and statistical signal processing with a focus on wireless communications networks.

Liang Chen received his B.E. degree from Zhejiang University, China, in 2003, and the M.S. degree from the University of Melbourne, Australia, in 2006, where he is currently a PhD candidate. He was the recipient of best paper awards from the 2006 Australian Communications Theory Workshop and the 2006 European Wireless Conference, respectively. During the winter of 2010, he worked at National Institute of Informatics, Japan, as a visiting researcher. In 2011, he also received a Victoria Fellowship from the Victoria State Government of

Brian Krongold received his B.S., M.S., and Ph.D. degrees in electrical engineering in 1995, 1997 and 2001, respectively, from the University of Illinois at Urbana-Champaign, and worked as a Research Assistant at the Coordinated Science Laboratory from 1995–2001. From December 2001 to December 2004, he was a Research Fellow in the ARC Special Research Centre for Ultra-Broadband Information Networks in the Department of Electrical and Electronic Engineering at the University of Melbourne, Australia. He was awarded an ARC Postdoctoral

Jamie Evans was born in Newcastle, Australia, in 1970. He received the B.S. degree in physics and the B.E. degree in computer engineering from the University of Newcastle, in 1992 and 1993, respectively, where he received the University Medal upon graduation. He received the M.S. and the Ph.D. degrees from the University of Melbourne, Australia, in 1996 and 1998, respectively, both in electrical engineering, and was awarded the Chancellors Prize for excellence for his Ph.D. thesis. From March 1998 to June 1999, he was a Visiting Researcher in the